

Carbides in Co-17Re-23Cr-xTa-2.6C –based (x=0, 1.2) high temperature alloys

N. Wanderka¹, M.S. Mousa², P. Henke¹, O. Korchuganova^{1,3}, D. Mukherji⁴, J. Rösler⁴, J. Banhart¹

¹Helmholtz-Zentrum Berlin für Materialien und Energie, Hahn-Meitner 1 Platz 1, 14109 Berlin, Germany

²Mu'tah University, Department of Physics, Al-Karak, Jordan

³National Research Nuclear University «MEPhI», Moscow, 115409, Russian Federation

⁴Technische Universität Braunschweig, Institut für Werkstoffe, 38106 Braunschweig, Germany

Abstract

Co-Re-base alloys with very high melting point are being developed to supplement Ni-superalloys in future gas turbines in which much higher gas entry temperatures are expected. The microstructure of two Co-17Re-23Cr-2.6C and Co-17Re-23Cr-1.2Ta-2.6C alloys has been investigated by scanning and transmission electron microscopy but it is not trivial to accurately quantify the composition of the carbides. The compositions of various carbides in Co-Re-base alloys were quantified with near-atomic resolution using atom probe tomography. It was found that Cr as well as Ta form carbides with different morphologies and size ranging from extremely fine (nm scale) to large (μm scale). The composition and the crystal structure of the investigated phases are reported. It has been shown that Ta carbides are more stable than Cr-rich carbides at temperatures of 1200°C after long time ageing. They are also effective strengthening precipitates.

Key words: Co-based alloys, carbides, microstructure, transmission electron microscopy, atom probe tomography

The corresponding author: wanderka@helmholtz-berlin.de

1. Introduction

Along with Ni-based superalloys, Co-base superalloys have been used in gas turbine applications since the 1940s (Sullivan *et al.* 1970). Due to their lower strength Co-base alloys are mainly used as static components (e.g. vanes), while Ni-superalloys, which experienced a tremendous development in the past 7 decades, are now the dominating material in the rotating components in the hot section of gas turbines. Presently, the application temperature of Ni-base superalloys is limited to about 1100 °C, which corresponds to 80% of the alloy's melting temperature and is much lower than the gas entry temperature in the turbine (which can be as high as 1500 °C). Single-crystalline Ni-base superalloy turbine blades are air cooled and also protected by thermal barrier coatings (TBC) to meet this gap. Therefore, the search for new materials for applications at higher temperatures in gas turbine continues. Recent developments in new Co-base alloys (Sato *et al.* 2006) are promising and particularly Co-Re-base alloys (Rösler *et al.* 2007) are potential candidates. Co-Re-base alloys have a significantly higher melting temperature compared to Ni-base superalloys (Mukherji *et al.* 2014) and are strengthened by carbides of the type $M_{23}C_6$ or MC depending on the alloying addition. Chromium is added to Co-Re alloys mainly to provide oxidation resistance but its affinity for carbon leads to the formation of $Cr_{23}C_6$ -type carbides. Furthermore, when tantalum is added to the alloy, it forms tantalum carbide (TaC). With suitable heat treatment, a very fine morphology of both types of carbide precipitates could be achieved in Co-Re alloys. It was found that the fine TaC precipitates interact with dislocation during high-temperature creep deformation thereby providing high temperature strengthening (Brunner *et al.* 2010). In-situ neutron and synchrotron measurements however, indicated that the $Cr_{23}C_6$ -type carbides are unstable at temperatures above 1000° C (Mukherji *et al.* 2010).

The microstructure of the Co-Re-Cr-Ta-C alloy system is very complex and importantly the precipitate morphologies can be altered by heat treatment. In the past the microstructure in various Co-Re alloys and the crystal structure of different phases present in them, e.g. the top phases, the borides and the carbides has been characterized in various studies. Along with microscopy, X-ray and neutron diffraction were widely used (Mukherji *et al.* 2010a, Mukherji *et al.* 2012). Analytical tools such as energy-dispersive spectroscopy (EDS) adapted to scanning electron (SEM) or transmission electron microscopes (TEM) and even methods such as Prompt Gamma Activation Analysis (PGAA) were used to determine compositions (Mukherji *et al.* 2013). PGAA in particular was useful to detect boron in Co-alloys even when present in very small amounts (in part per million - ppm). However, the detection of carbon poses a challenge. Quantification of Carbon in a Co-Re-Ta alloy is especially difficult with PGAA, as the neutron capture cross section of C is very low (0.0038 barn) compared to the other elements (Co, Re, Ta) which have cross sections typically 3 orders of magnitude higher (37 barn, 92 barn, 20 barn, respectively). The scattered γ photons elevate the baseline in the spectrum below every characteristic peak, which is why weak peaks from C cannot be detected next to strong peaks of the metallic elements Co, Re, Ta. Such analysis becomes even more difficult when the analyzed phases are dispersed in the microstructure on the submicron scale. Carbon is also difficult to quantify by TEM and SEM as the microscope chamber and the sample are constantly contaminated by C deposition during scanning with the electron beam. One of the methods which allow for a quantitative analysis of small precipitates with nearly atomic resolution is atom probe tomography (APT) (Blavette *et al.* 1993, Kelly *et al.* 2012). The present work is focused on the investigation of various carbides formed in two alloys Co-17Re-23Cr-xTa-2.6C (where, $x = 0$ or 1.2)¹. For this, a combination of high-resolution methods has been used. The crystal structures of the various phases were first investigated by electron diffraction in the TEM, while the chemical composition was

¹ All compositions are given in atomic percentage unless otherwise specified.

analyzed by APT. This is the first report on the analysis of carbides in the Co-Re alloys by atom probe. On the other hand, simple tools like hardness measurements were used in this study to show the strengthening effects of the carbides. Microhardness is an effective indicator of their strength in the Co-Re alloys.

2. Experimental

Two alloys with nominal compositions Co-17Re-23Cr-2.6C and Co-17Re-23Cr-1.2Ta-2.6C (at.%) were prepared from high-purity metals and carbon powder (> 99.8 % purity) by melting in a vacuum arc furnace and cast into a solid copper mold. The cast bars (10 mm diameter) were homogenized (solution heat treated) in a vacuum furnace at 1350 °C for 7.5 h and at 1400 °C for 7.5 h followed by argon quenching. Both alloys have undergone heat treatments at 1000°C and 1200°C up to 1000 h. The alloy compositions were measured using EDS in the SEM at low magnification covering a large sample area.

Samples for TEM were prepared in two steps. First, square pieces of about $1.5 \times 1.5 \text{ mm}^2$ were mounted on a molybdenum ring of 3 mm diameter and mechanically thinned down to a thickness of about 20 μm . In the second step, the samples were milled by Ar-ions in a RES101 (BAL-TEC Company) at a voltage of 5 kV and a current of 2 mA to achieve electron transparency. The microstructure of the alloy investigated was characterized by a Philips CM30 TEM operating at 300 kV and equipped with an EDS detector. The EDS system was used for the determination of the chemical composition of different phases present in the alloy. A focused beam with a probe size of 10 nm was used for the analysis. The composition of phases reported in this paper is an average of 10 measurements on each phase. Selected area electron diffraction (SAD) was used for the measurement of the lattice parameters of the different phases.

For APT measurements square rods of $0.2 \times 0.2 \times 12 \text{ mm}$ were cut from the heat treated alloy. Sharp needle-shaped specimens were electrochemically polished in a 70% Methanol, 20% Glycerol (C₃H₈O₃) and 10% Perchloric acid solution at room temperature and a voltage of 6 V. The APT analyses were performed at a temperature of 70 K with a 20% pulse fraction and a pulse repetition rate of 1 kHz. An atom probe (TAP, CAMECA) was employed in this study (Blavette *et al.* 1993).

Macrohardness measurements were carried out on a testing machine from Zwick using a diamond pyramid indenter and an applied load of 98.1N to obtain the Vickers Hardness Number (HV). Five tests were conducted for each measurement with a loading time of 15 s. Additionally, microhardness testing was performed with a MHT-4 testing machine from Anton Paar, fitted with a square-base diamond pyramid indenter, to measure the hardness of the different phases present in the alloys. Measurements were performed with smaller loads of 0.025 to 0.05 N and 30 s loading time. The microhardness values are also reported as Vickers hardness numbers (HV) and are the average value from 5 measurements.

3. Results and discussion

The alloy composition analyzed by EDS in SEM was quantified in two ways, considering either the absence of C or its presence in the alloys (Table 1). It is seen that while the accuracy in the quantification of metallic elements (Re, Cr and Ta) in the three alloys by EDS is reasonable (especially when C is not included in the analysis) and the results are close to the nominal compositions, the quantification of C by EDS is quite erroneous. The values of 12.13 C for the alloy with Ta and 7.65 for the alloy without Ta (Table 1) is too high compared to the nominal values of 2.6. This error becomes more obvious if one considers the result of

the wet-chemical analysis on the alloy Co-17Re-1.2Ta-1.08C, having similar composition like the two alloys investigated in this study. This alloy was processed and heat treated in the same way as the alloys Co-17Re-23Cr-xTa-2.6C under investigation. The EDS measurement again shows high C values (7.44 compared to a nominal value of 1.08), but the wet-chemical analysis (1.022 C) matches the nominal composition and shows that there is only a minimal loss of alloying elements during the method adopted for the processing of Co-Re alloys. The values measured by wet-chemical analysis are in wt. % (also the % error is reported in Table 1). The reported at.% values are calculated from the measured values. Although wet-chemical analysis may be used with some success for carbon quantification in Co alloys, it is destructive and unlike EDS in SEM, does not provide spatially resolved information, which would be useful for the analysis of fine structures. Therefore, it is not possible to use this method for carbon analysis of finely dispersed precipitates in the alloy. Atom probe was therefore used for the analysis of various carbides in the Co-Re alloys.

SEM and TEM investigations of the carbide morphology

Low magnification SEM micrographs of the Co-17Re-23Cr-2.6C and Co-17Re-23Cr-2.6C-1.2Ta alloys are shown in Fig. 1. It is interesting to note that an addition of only 1.2 at. % Ta to Co-17Re-23Cr-2.6C can make such a drastic change in the microstructure (compare both alloys in Figs. 1a and 1b). The alloy without Ta contains mainly Cr-carbide (dark grey contrast) in different morphologies and various length scales (Fig. 1a). Figure 1a shows a typical microstructure of a polycrystalline alloy that contain massive Cr_{23}C_6 -type carbides at the grain boundaries (gb) and blocky Cr_{23}C_6 particles ($> 1\mu\text{m}$) within the grains. In contrast, the alloy with Ta addition shows presence of huge Cr-Re-rich σ phase particles (bright grey contrast) in Fig. 1b. What is not seen in the low magnification SEM micrograph is that the matrix in Fig. 1a additionally contains Cr_{23}C_6 lamellae, which are better resolved in Fig. 2a. Figure 2b clearly shows different phases (σ and Ta-carbides) with different contrast when imaged with the annular backscattering detector (CBS). The σ phase and the TaC phase are easily distinguished by their light grey (σ) and very bright (TaC) contrasts. Several large rounded σ phase particles (diameter $> 10\mu\text{m}$) are located at the grain boundaries along with smaller globular particles (size $< 10\mu\text{m}$) showing the same contrast and distributed inside the grains. The σ phase is enriched in Re and depleted in Co. A detailed analysis of σ phase has already been reported previously in Refs. (Mukherji *et al.* 2010a, Mukherji *et al.* 2012). The σ phase has a tetragonal structure (space group #136: P 42/m n m) and its composition slightly varies depending on the alloy composition. In the present alloy, the lattice parameters were determined by selected-area electron diffraction to $a = 0.9003\pm 0.003\text{ nm}$ and $c = 0.5098\pm 0.002\text{ nm}$, which generally agrees with other investigated alloys (Depka *et al.* 2014, Paulisch *et al.* 2013). In this work, more attention is paid to the analysis of different carbides present in the alloys. TaC carbides are located at the grain boundaries, at the interfaces of the σ phase (marked by black arrows) and some also in the grain interior.

The spherical TaC particles marked in Fig. 2b are mostly smaller than the σ phase particles. The magnified secondary electron (SE) SEM image of Co-17Cr-23Re-1.2Ta-2.6C alloy in Fig. 2c shows the lamellar structure, which could not be resolved in Fig. 2b. The lamellae are rich in Cr and C as in the alloy without Ta and have been identified as Cr_{23}C_6 phase. In Fig. 2c, one also finds a very fine dispersion (30 to 50 nm) of precipitates rich in Ta and C.

Fig. 3 shows TEM images of the fine lamellae structure that are present in both the alloys. In the alloy without Ta, long thin plates are oriented nearly parallel and have a thickness of the order of 40 nm and an inter-plate distance varying between 200 to 500 nm (Fig. 3a). Composition measurement (quantitative) on the thin plates was difficult but selected area diffraction (SAD) analysis in TEM identified the lamellae as Cr_{23}C_6 -type carbides having

space group #225: $Fm\bar{3}m$ (Fig. 3a inset). The $M_{23}C_6$ precipitates and the Co-matrix show an orientation relationship of type $(111) M_{23}C_6 \parallel (0001) \text{ hcp Co}$, $[0\bar{1}1] M_{23}C_6 \parallel [10\bar{1}0] \text{ hcp Co}$ and $(211) M_{23}C_6 \parallel (0\bar{1}10) \text{ hcp Co}$ and the carbide plates are semi-coherently embedded in the matrix. Fig. 3b shows a bright-field TEM image of the lamellar precipitates in the Co-17Re-23Cr-1.2Ta-2.6C alloy. They are also semi-coherently embedded into the Co matrix but are sometime broken down and discontinuous (see also Fig. 2c). The SAD pattern from the plate-like precipitates along the $[1-23]$ zone axis is shown in the inset of the Fig. 3b. The diffraction pattern suggests a lattice parameter $a = 1.103 \pm 0.009$ nm and therefore, these Cr and C rich precipitates are $M_{23}C_6$ type Cr carbide according to the lattice parameter.

In the alloy with Ta, ~ 500 nm precipitates (rich in Ta and C) with globular or rhombohedral morphologies are also imaged with TEM and shown in Fig. 4a and 4b. The corresponding SAD along the $[011]$ and $[001]$ zone axes are shown in the inset, respectively. This phase also has a cubic structure (space group #225: $Fm\bar{3}m$) with the lattice parameter $a = 0.444 \pm 0.002$ nm. In the binary Ta-carbide this value of lattice size corresponds to the nonstoichiometric TaC_y with C / Ta ratio $y = 0.9$ (Mukherji *et al.* 2010). Along with the large Ta-rich precipitates there are many small precipitates marked by arrows in Fig. 4b which are also enriched in Ta. All precipitates in Fig. 4 were identified as TaC. Since carbon cannot be accurately quantified by TEM/EDS, the identification of carbides was mainly based on the crystal structure / lattice size and the presence of the metallic element Cr or Ta.

APT of carbides

An accurate chemical analysis of all elements on precipitates dispersed on the nm-scale still up to date is the main objective of many investigations by APT (Timochina *et al.* 2007, Mulholland *et al.* 2011, Seol *et al.* 2013, Yuan *et al.* 2012, Wanderka *et al.* 1994, Delargy *et al.* 1983). This technique has been used to quantify carbon in the carbides of different types in different steels and in Ni-based superalloys. For example, in an advanced high-strength low-alloy steel two types of very small size (radius in the range of 1.5 and 2 nm) $Ti_{0.98}Mo_{0.02}C_{0.6}$ and MoC (with partial substitution of Mo by Cr) carbides could be found along the γ/α interface by atom probe (Timochina *et al.* 2007). Further, quantification of carbon in M₂C type carbides in high-strength low carbon steel (in which M represents a combination of metallic elements) has also been performed by APT, but the amount of carbon measured did not correspond to the stoichiometric composition (Mulholland *et al.* 2011). The authors suggested that the deviation in the composition of M₂C was due to trajectory overlap effect that arises because of field evaporation differences of the matrix and the precipitates in APT measurement. Similar quantification problem of the nanoscale κ -carbide was also reported for APT measurement in Fe-Mn-Al-C alloy (Seol *et al.* 2013). On the other hand the carbon content of 25.1 at% in the M₃C carbide measured by APT in ultra-high strength ferritic stainless steel indicated cementite stoichiometry (Yuan *et al.* 2012). This means that the local magnification effect appears as an APT artifact, which is particularly strong for measurements of very small precipitates. In an earlier measurement we presented quantitative analyses of large about 100 nm sized $M_{23}C_6$ carbides in MANET steel after simultaneous irradiation / He⁺ ion implantation where the amount of measured carbon corresponded to the stoichiometric composition (Wanderka *et al.* 1994). The composition and stability of phases in various Ni-base superalloys, including analysis of MC and $M_{23}C_6$ carbides has been also investigated in IN939 (Delargy *et al.* 1983). This clearly showed that atom probe is an effective tool for the characterization of carbides in steels, Ni- and Co-base alloys but needs to be applied with some care, particularly when the precipitates are very small (Blavette *et al.* 1996).

In the present study, the chemical composition of carbides in the Co-Re-base alloys was measured by APT. Figure 5 (a-e) displays the reconstruction of Co, Cr, Re, Ta and C atom positions in an investigated volume of $13 \times 13 \times 38 \text{ nm}^3$. All alloying elements are distributed non-uniformly and form three distinct regions within this reconstructed volume. The first region is mainly enriched in Cr and C and depleted in Co. The second region is Ta and C rich and, the third region is enriched in Co and Re but also containing notable amounts of Cr. The phases shown here can be identified as Cr carbide, Ta carbide and the Co matrix. The concentration depth profiles in Fig. 5f are taken along the cylinder of 1 nm radius shown in Fig. 5a. All the three regions are clearly distinguishable in the depth profile. The chemical compositions of the phases were however, not calculated from depth profiles, but from the larger measured volume to improve statistics and to increase the accuracy of the analysis. Concentration of Carbon was calculated from single, double and complex charged ions ($^{12,13}\text{C}^+$ at 12, 13 amu, $^{12,13}\text{C}^{2+}$ at 6, 6.5 amu and $2(^{12,13}\text{C}^+)$ at 24, 26 amu). Chromium atoms evaporated exclusively in the doubly charged state ($^{50}\text{Cr}^{2+}$, $^{52}\text{Cr}^{2+}$, $^{53}\text{Cr}^{2+}$, $^{54}\text{Cr}^{2+}$). Rhenium atoms were detected as doubly and trebly charged ions ($^{185,187}\text{Re}^{3+}$ at 62.3, 63.3 amu and $^{185,187}\text{Re}^{2+}$ at 92.5, 93.5 amu). Tantalum was calculated from trebly and quadruple charged ions ($^{181}\text{Ta}^{3+}$ at 90.5 amu and $^{181}\text{Ta}^{4+}$ at 45.25 amu). No significant peak at 90 amu or 45 amu from ^{180}Ta (0.01%) isotope has been obtained. Single charged oxygen as $(\text{H}_2\text{O})^+$ appeared in small amounts in the mass spectrum (not shown here) at 18 amu has also been measured. No overlap of any peaks of detected elements has been measured in the investigated alloy. The average compositions of carbides are given in Table 2.

From the values it can be seen that the chemical composition of Cr carbide corresponds to the composition $(\text{CrReCoTa})_{77.6}\text{C}_{22.4}$, which is close to a M_{23}C_6 type. The observed Cr carbide is not present as pure Cr_{23}C_6 but the metallic (M) content of the carbide phase is mainly composed of Cr, Co and Re. This is not surprising considering the heavy presence of these elements in the Co-Re alloy investigated. For example, it was reported that depending on the composition of steels and Ni-base superalloys, the metallic (M) content of M_{23}C_6 type carbides may contain elements like Fe, Mo, etc. beside Cr (Hättestrand et al. 1999, Hofer et al. 2000). In the present alloy, Co and Re are dissolved in Cr_{23}C_6 in substantial amounts. Small amounts of Ta and O ($< 1 \text{ at. } \%$) are also detected in the investigated Cr carbide. The composition of M_{23}C_6 type carbides was measured four times and the average value is reported in the Table 1. In the present measurements, the magnification effect seems not to be significant and does not influence the results significantly. Most probably this is because relatively large size of M_{23}C_6 (lamellae of $\sim 20 \text{ nm}$ thick) carbides were measured in the present work (Fig. 2). Other types of Cr-rich carbides (e.g. M_2C , M_6C or M_7C_3 , etc.) were not found in Co-17Re-23Cr-1.2Ta-2.6C, but Ta carbides have been identified in this alloy by 3D-APT, as well. The composition of the Ta carbide correspond to $(\text{TaReCoCr})_{48}\text{C}_{52}$, i.e. the MC type carbide. Considering the uncertainty of more than $\pm 2\%$ in the estimation of C and Ta in this measurement it is difficult to conclude if the carbide is stoichiometric or nonstoichiometric. From the binary Ta-C system it is however, well known that TaC is a strongly nonstoichiometric interstitial compound with y ranging between 0.6 to 1 (Mukherji *et al.* 2010). In the MC phase more than 52 at. % C has been measured while less than 10 at. % of Ta is substituted by Co, Cr or Re. The value of y in $(\text{TaReCoCr})_{48}\text{C}_{52}$ is then greater than 1 ($y = 1.08$) which extends beyond the range of y in binary TaC_y . In this special case Ta carbide is located between the M_{23}C_6 carbide and the matrix. The morphology of the Ta carbide is most probably plate-like with a thickness of about 3 nm. Here we would therefore, expect a trajectory overlap effect during measurement. Assuming that it takes place from the matrix, the amount of Co should be the highest in TaC carbide and this is in fact the case (2.82 at.%). Based on the same consideration, the amount of Cr (1.49 at.%) should be higher than of Re (2.56 at.%) but this is not the case. Since the field-evaporation and the local magnification or demagnification of all phases is not known, it is difficult to judge which phase (M_{23}C_6 or

matrix) influences the composition of TaC. The oxygen content in the Ta carbide is very small, much less than that measured in the Cr carbide. The Co-matrix contains ~ 19 at.% Cr and > 17 at.% Re (see Table 1) and from the SAED measurement the Co matrix was found to have a hexagonal structure with lattice parameter $a = 0.2566$ nm and $c = 0.4136$ nm.

Hardness measurements: strengthening by carbides

A simple hardness measurement was used to determine the strengthening potential of the fine dispersion of carbides in the alloys with and without Ta addition. Fig. 6a shows the indentation marks from a microhardness measurement in the Co-17Re-23Cr-2.6C alloy in two heat treatment conditions, where in one condition the Cr_{23}C_6 lamellar are present (right image) and in the other condition when they are absent (left image) in the Co-matrix. The measured hardness values (803 and 690 HV) are also indicated in the picture and it clearly shows a significant hardening in the alloys due to the fine lamellar carbides. Fig. 6b plots the hardness evolution on the samples when the two alloys were exposed to high temperatures (1000° and 1200°C) up to 1000 hours. Firstly, if one compares the 0 hour exposure values (which represents the hardness in ST conditions for the two alloys, it is noticed that the alloy with Ta has a higher hardness value. Clearly, in addition to the strengthening effect due to the fine lamellar Cr-carbides, the even finer dispersion of TaC precipitates in the alloy containing Ta provides additional strengthening. The plot in Fig. 6b further shows that this strengthening remains stable in the alloy even after a very long exposure at 1000°C. In contrast, the Cr-carbides are less stable and significant loss of strength is observed on exposure at 1000° and 1200°C even after 100 hours. A similar loss is also observed, but to a lesser extent, in the alloy with Ta. Earlier in-situ neutron and synchrotron measurements in the alloy without Ta had shown that Cr carbide tends to dissolve and the freed Cr combines with the Re in the matrix to form σ phase after a few hour of exposure at 1000°C (Mukherji *et al.* 2010). On the other hand recent diffraction and small angle scattering measurements at high temperatures shows that TaC remain stable at 1200°C and above (Mukherji *et al.* 2013).

Summary

A combination of scanning electron microscopy, transmission electron microscopy and atom probe tomography has been used for the study of carbides in Co-17Re-23Cr-2.6C and Co-17Re-23Cr-1.2Ta-2.6C alloys. Carbides have been characterized according to their morphology, structure and chemical composition. Cr-rich M_{23}C_6 type of carbides with different morphology but with the same structure has been found in the Co-17Re-23Cr-2.6C alloy. Co-17Re-23Cr-1.2Ta-2.6C alloy beside the Cr-rich carbides consists of σ phase and a second type of carbides, namely Ta-rich MC type. In the Cr-carbides the measured chemical composition deviates from the stoichiometric composition but it is not clear about this in the Ta-carbide. For the Cr_{23}C_6 type carbides nearly 29 at. % of M is substituted, mainly by Co (~ 15.2 at. %) and Re (~ 11.0 at. %), with small amounts each (< 1 at. %) of Ta and O. In TaC carbide, the measured Ta content was greater than 40 at. % and ~ 7 at. % of M is substituted by Co, Cr and Re. The crystal structures of both the carbides are cubic and correspond to the known carbide structures of Cr and Ta respectively: i.e. fcc with lattice parameters $a = 1.103 \pm 0.009$ nm for Cr_{23}C_6 and $a = 0.444 \pm 0.002$ nm for TaC (which matches the lattice size of TaC_y with $y = 0.9$ of the binary phase). Unlike other Co-base alloys, the hcp Co structure is stabilized at room temperature by the addition of Cr and Re in the Co-17Re-23Cr-1.2Ta-2.6C alloy, as both Re and Cr are hcp stabilizer in Co. Fine dispersed carbides contribute to the strengthening effect of the alloys. However, the alloy with additions of Ta demonstrates

higher strengthening effect as that without Ta. The strengthening remains stable in both alloys even after a very long exposure at 1000°C. However, at 1200°C the Cr-carbides are less stable as Ta-carbides and significant loss of strength has been observed.

Acknowledgements:

The authors would like to thank the German Research Foundation (DFG) for providing the financial support under the contract number RO 2045/31-1 at the TU Braunschweig. One of the authors would like to thank the Alexander von Humboldt Foundation for financial support to do research at the HZB.

References

- Sullivan, P.C., Donachie, M.J. and Morral, F.R. (1970) “Cobalt-Base Superalloy-1970”, Cobalt Monograph Series (Cobalt Information Center, Brussels).
- Sato, J., Omori, T., Oikawa, K., Ohnuma, I., Kainuma, R., and Ishida, K. (2006) “Cobalt-Base High-Temperature Alloys”, *Science* 312, 90–91.
- Rösler, J., Mukherji, D. and Baranski, T. (2007) “Co-Re-based Alloys: A New Class of High Temperature Materials?”, *Adv. Eng. Mater.* 9, 876–881.
- Mukherji, D., Gilles, R., Karge, L., Strunz, P., Beran, P., Eckerlebe, H., Stark, A., Szentmiklosi, L., Mácsik, Z., Schumacher, G., Zizak, I., Hofmann, M., Hoelzel M. and Rösler, J. (2014) “Neutron and synchrotron probes in the development of Co-Re-based alloys for next generation gas turbines with an emphasis on the influence of boron additives”, *J. Appl. Cryst.* 47, 1417–1430.
- Brunner, M., Hüttner, R., Bölit, M.-C., Völkl, R., Mukherji, D., Rösler, J., Depka, T., Somsen, C., Eggeler G. and Glatzel, U. (2010) “Creep properties beyond 1100°C and microstructure of Co-Re-Cr alloys”, *Mat. Sci. Eng. A* 528, 650–656.
- Mukherji, D., Klauke, M., Strunz, P., Zizak, I., Schumacher, G., Wiedenmann, A. and Rösler, J. (2010) “High temperature stability of Cr-carbides in an experimental Co-Re-based alloy”, *Int. J. Mat. Res.* 101, 340-48.
- Mukherji, D., Strunz, P., Gilles, R., Hofmann, M., Schmitz, F. and Rösler, J. (2010a) “Investigation of phase transformations by in-situ neutron diffraction in a Co-Re-based high temperature alloy”, *J. Mater. Lett.* 64, 2608–2611.
- Mukherji, D., Strunz, P., Piegert, S., Gilles, R., Hofmann, M., Hoelzel, M. and Rösler, J. (2012) “The Hexagonal Close-Packed (HCP) \rightleftharpoons Face-Centered Cubic (FCC) Transition in Co-Re-Based Experimental Alloys Investigated by Neutron Scattering”, *Metall. Mater. Trans. A*, 43, 1834–1844.
- Mukherji, D., Rösler, J., Wehrs, J., Strunz, P., Beran, P., Gilles, R., Hofmann, M., Hoelzel, M., Eckerlebe, H., Szentmiklósi, L. and Mácsik, Z. (2013) “Application of In Situ Neutron and X-Ray Measurements at High Temperatures in the Development of Co-Re-Based Alloys for Gas Turbines”, *Metall. Mater. Trans. A* 44, 22–30.
- Blavette, D., Deconihout, B., Bostel, A., Sarrau, J. M., Bouet M. and Menand, A. (1993), “The Tomographic Atom-Probe: a quantitative three-dimensional nanoanalytical instrument on a nearly atomic-scale”, *Rev. Sci. Instrum.* 64, 2911–2919.
- Kelly, T. F., Larson, D. J. (2012), “Atom probe tomography 2012”, *Annu. Rev. Mater. Res.* 42, 1-31.
- Depka, T., Somsen, C., Eggeler, G., Mukherji, D. and Rösler, J. (2014) “Sigma phase evolution in Co-Re-Cr-based alloys at 1100°C”, *Intermetal.* 48, 54–61.
- Paulisch, M., Wanderka, N., Mieke, G., Mukherji, D., Rösler, J. and Banhart, J. (2013), “Characterization of borides in Co-Re-Cr-based high-temperature alloys”, *J. Alloy & Compd.* 569, 82–87.
- Timochina, I.B., Hodson, P.D., Ringer, S.P., Zheng R.K. and Pereloma, E.V. (2007), “Precipitate characterization of an advanced high-strength low-alloy (HSLA) steel using atom probe tomography”, *Scr. Mater.* 56, 601-604.
- Mulholland, M.D. and Seidman, D.N. (2011), “Nanoscale co-precipitation and mechanical properties of a high-strength low-carbon steel”, *Acta Mater.* 59, 1881-1897.
- Seol, J.-B., Raabe, D., Choi, P., Park, H.-S., Kwak J.-H. and Park, C.-G. (2013), “Direct evidence for the formation of ordered carbides in a ferrite-based low-density Fe-Mn-Al-C alloy studied by transmission electron microscopy and atom probe tomography”, *Scr. Mater.* 68, 348-353.

- Yuan, L., Ponge, D., Wittig, J., Choi, P., Jimenez, J.A. and Raabe, D. (2012), "Nanoscale austenite reversion through partitioning, segregation and kinetic freezing: Example of a ductile 2 GPa Fe–Cr–C steel", *Acta Mater.* 60, 2790-2804.
- Wanderka, N. and Wahi, R.P., (1994), „An AP/FIM and TEM study of the microstructural evolution of MANET steel after dual-beam irradiation", *Appl. Surf. Sci.* 76/77, 272-277.
- Delargy, K.M. and W. Smith, G.D. (1983), "Phase composition and phase stability of a high-chromium nickel-based superalloy, IN939", *Metall. Mater. Trans. A*, 14, 1771–1783.
- Blavette, D., Duval, P., Letellier, L. and Guttmann, M. (1996), "Atomic-scale APFIM and TEM investigation of grain boundary microchemistry in Astroloy nickel base superalloys", *Acta Mater.* 44, 4995-5005.
- Hättestrand, M. and Andrén, H.-O. (1999), "Boron distribution in 9-12% Cr steels", *Mat. Sci. & Eng. A* 270, 33–37.
- Hofer, P., Miller, M. K., Babu, S. S., David, S. A. and Cerjak, H. (2000), "Atom probe field ion microscopy investigation of boron containing martensitic 9 Pct chromium steel", *Metall. Mater. Trans. A*, 31, 975–984.

Figure captions

Fig. 1. SEM micrographs of: a) Co-17Re23Cr-2.6C alloy. Cr_{23}C_6 carbides (dark grey contrast) are embedded in the matrix. b) Co-17Re23Cr-1.2Ta-2.6C alloy in ST condition. TaC carbides are imaged by very bright contrast, σ phase is light grey.

Fig. 2. SEM images of polycrystalline a) Co-17Re23Cr-2.6C alloy in ST condition, Lamellar and blocky Cr_{23}C_6 carbides are marked; b) and c) Co-17Re23Cr-1.2Ta-2.6C alloy in ST condition. The low magnification image in b) with CBS detector shows light grey contrast for the σ phase (marked σ) and bright contrast for TaC phase (marked by black arrows). The higher magnification SE image in c) resolves the matrix substructure as lamellar Cr_{23}C_6 carbides and a very fine dispersion of TaC precipitates between the lamellae.

Fig. 3. Bright field TEM images of plate-shaped precipitates embedded in the matrix of: a) Co-17Re23Cr-2.6C alloy in ST condition; selected area diffraction pattern of the matrix with the $[0\bar{1}10]$ zone axis and of the Cr_{23}C_6 carbides ($[211]$ zone axis) is in the inset. b) Co-17Re23Cr-1.2Ta-2.6C alloy in ST condition. The SAD pattern of a plate-shaped precipitate oriented along the $[1\bar{2}3]$ zone axis is shown in the inset.

Fig. 4. Bright-field TEM images of precipitates enriched in Ta and C with globular or rhombohedral morphology in Co-17Re-23Cr-1.2Ta-2.6C alloy are shown in (a) and (b), respectively. The corresponding SAED patterns along the $[011]$ and $[001]$ zone axes are shown in the inset. Many small precipitates marked by arrows in (b) are also enriched in Ta. All carbides are identified as TaC type.

Fig. 5. Three dimensional reconstruction of C: , Cr: , Ta: , Co: and Re: atom positions in an investigated volume $13 \times 13 \times 38 \text{ nm}^3$ of a Co-17Re-23Cr-1.2Ta-2.6C alloy. Three distinct regions are visible: Cr-rich, Ta-rich and Co-rich. A cylinder of 1 nm radius is marked in Fig. 5a along which concentration depth profiles were determined (Fig. 5b).

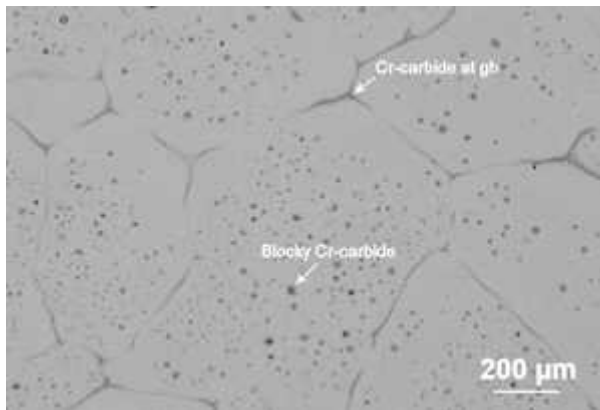
Fig. 6. a) SEM micrographs of Co-17Re-23Cr-2.6C alloy after ageing at $1000^\circ \text{C} / 100 \text{ h}$ (right image) and after ageing at $1200^\circ \text{C} / 100 \text{ h}$ (left image). b) Hardness evolution in alloys with and without Ta with exposure at 1100°C and 1200°C .

Tables

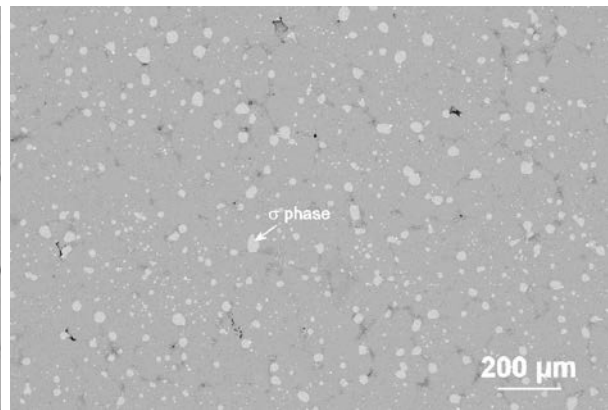
Table 1: Compositions of the two alloys measured by EDS in SEM. The evaluation is made in two ways considering either C is present or is absent in the alloys.

Table 2: Chemical compositions of different phases in Co-17Re-23Cr-1.2Ta-2.6C alloy measured by atom probe tomography. All values are given in at. %. The given error is 2σ deviation.

Figures:

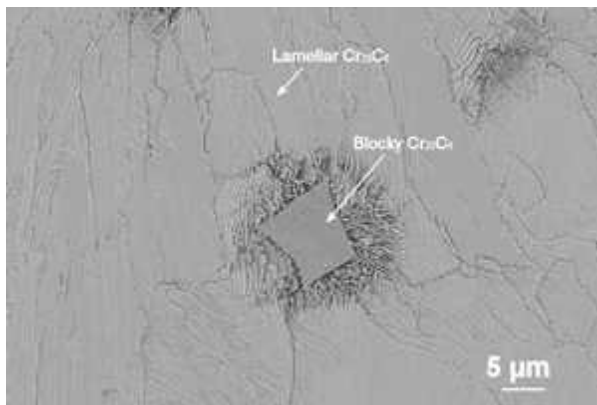


a)

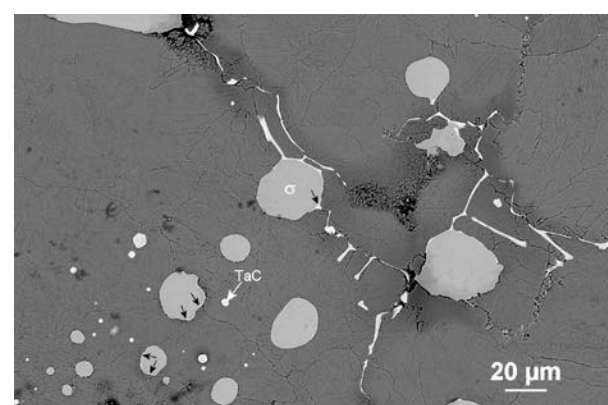


b)

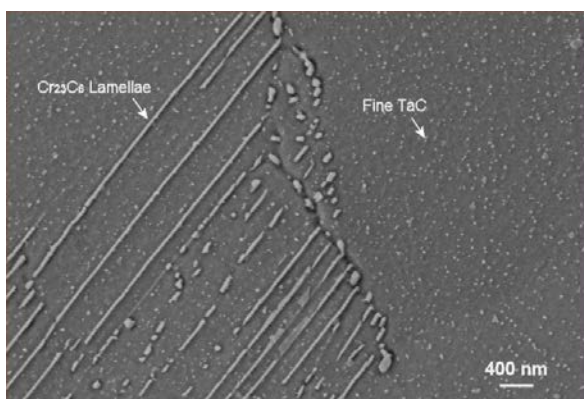
Fig. 1



a)

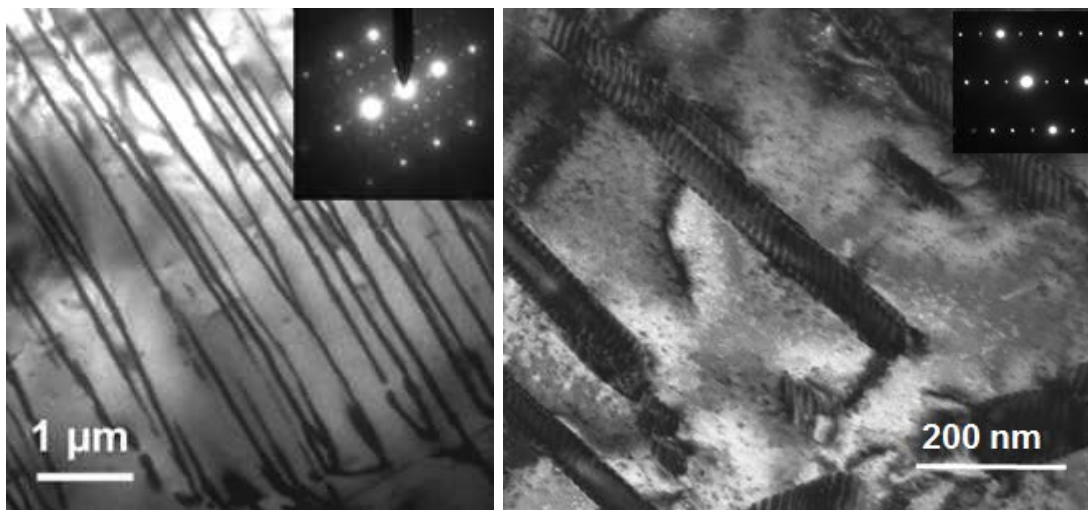


b)



c)

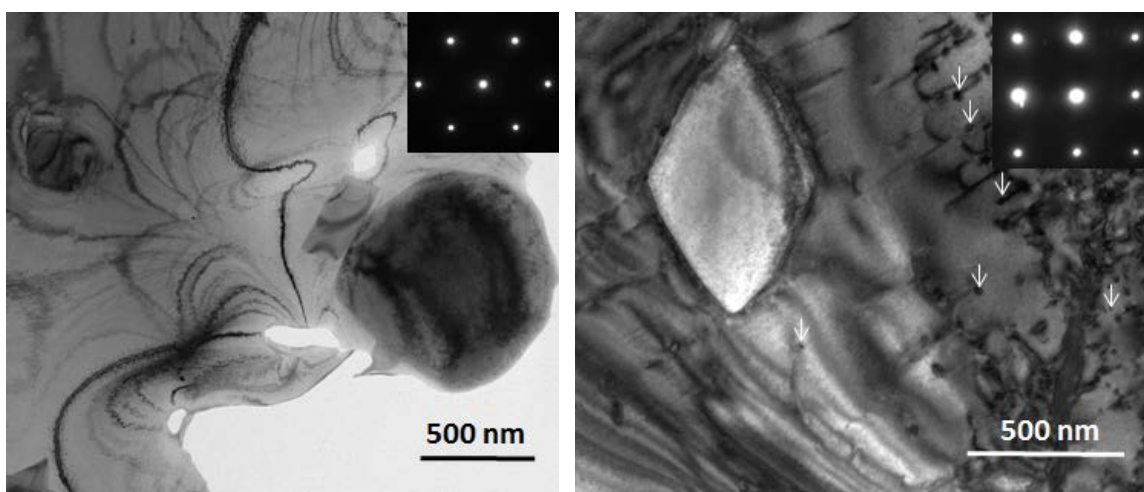
Fig. 2



a)

b)

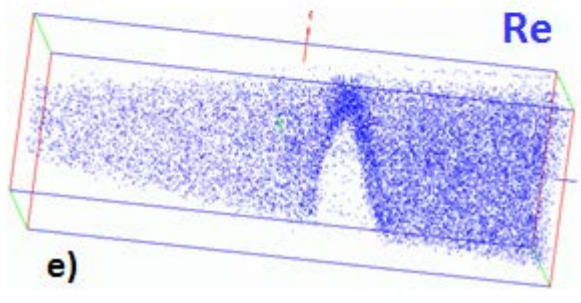
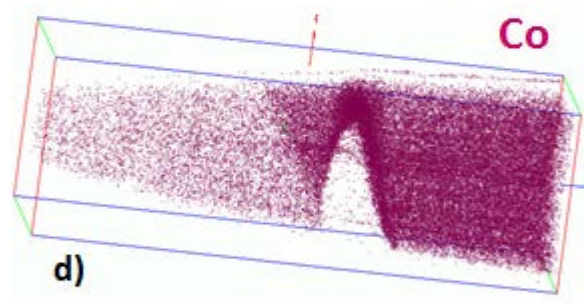
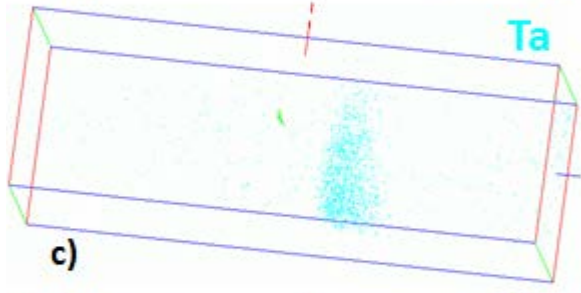
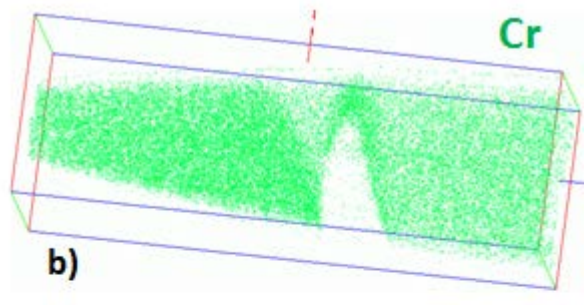
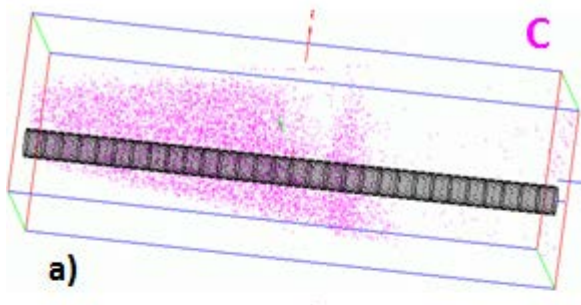
Fig. 3

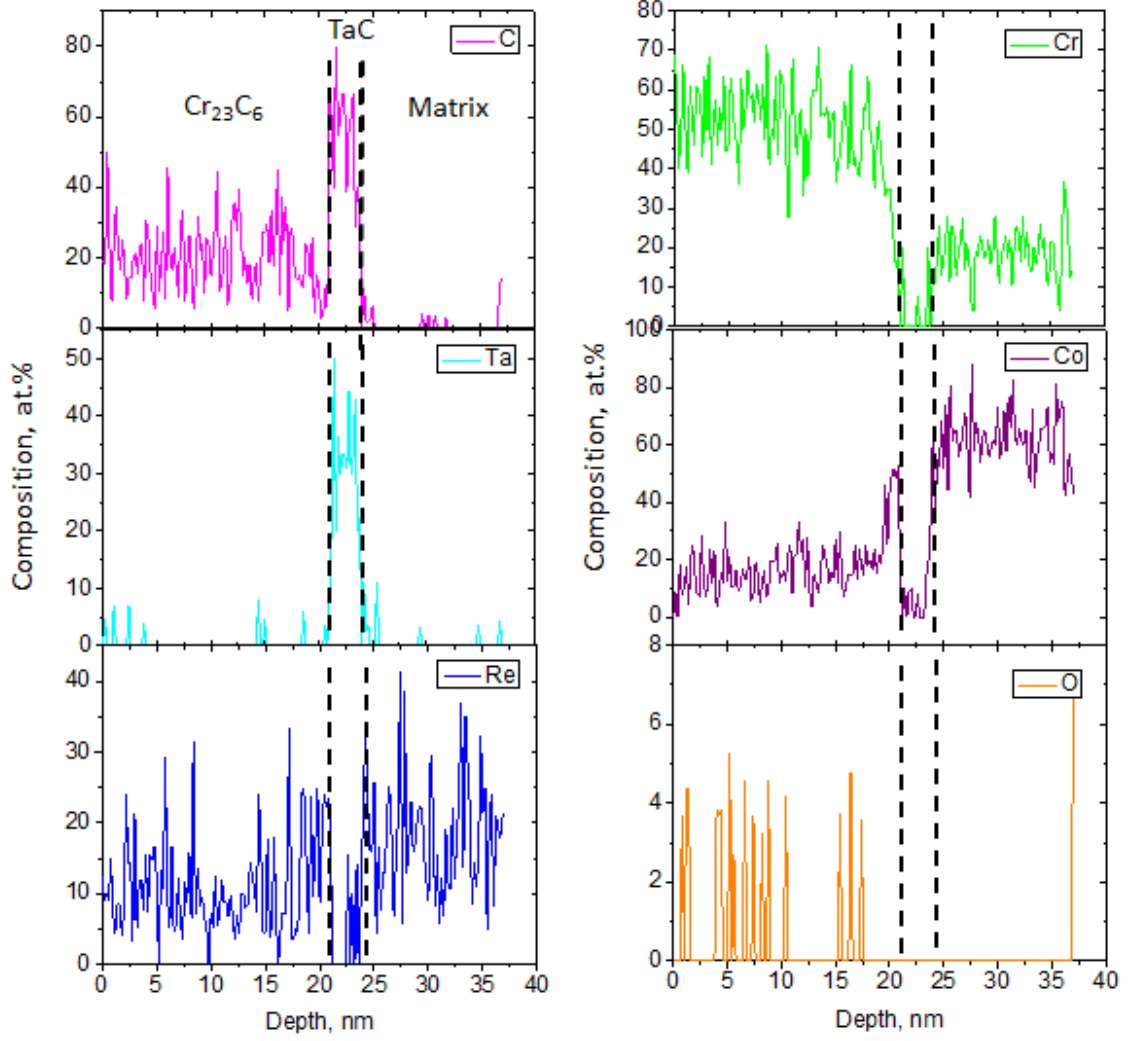


a)

b)

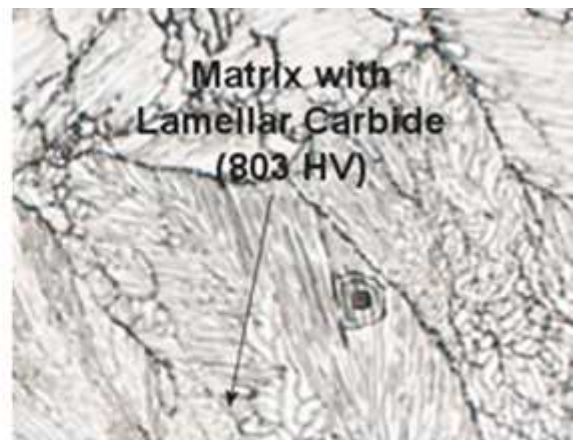
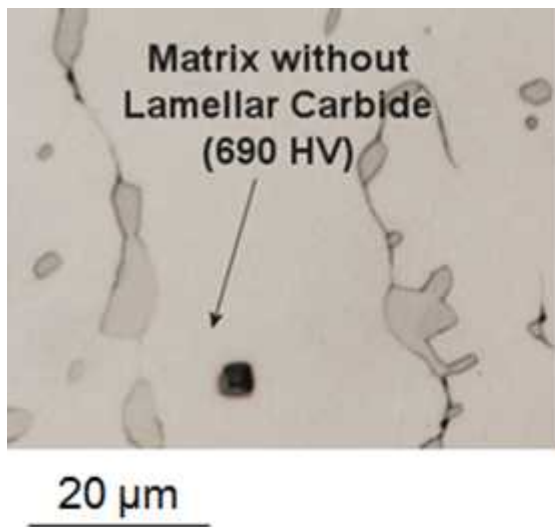
Fig. 4



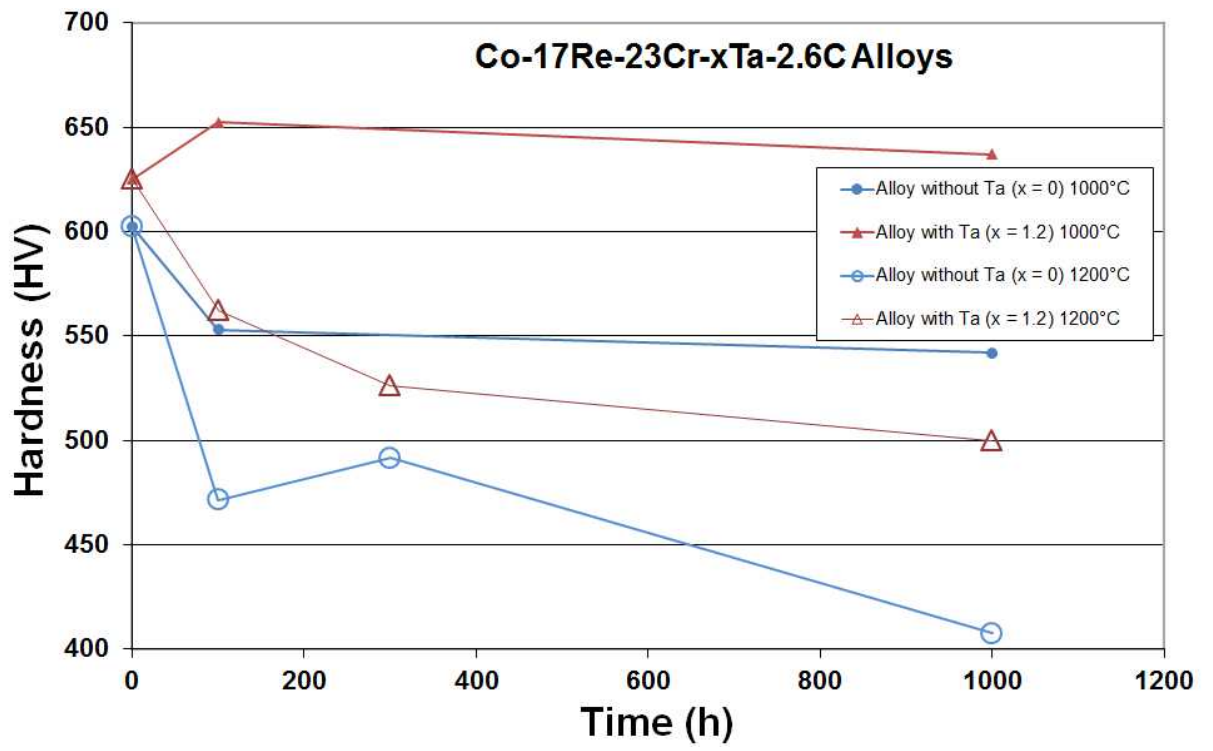


f)

Fig. 5



a)



b)
Fig. 6